



1

2 **Climatology of ionosphere over Nepal based on GPS TEC data from** 3 **2008 to 2018**

4

5

6 Drabindra Pandit^{1,6}, Basudev. Ghimire^{1,6}, Christine Amory-Mazaudier^{2,3}, Rolland Fleury⁴,
7 Narayan Prasad Chapagain⁵, Binod Adhikari⁶

8

9 1. Central Department of Physics, IOST, Tribhuvan University, Kathmandu, Nepal

10 2. Sorbonne Universités UPMC Paris 06, LPP, Polytechnique, France

11 3. T/ICT4D Abdus Salam ICTP, Italy

12 4. Lab-STICC, UMR 6285, Institut Mines-Telecom Atlantique, site de Brest, France

13 5. Amrit Campus, Tribhuvan University, Thamel, Kathmandu, Nepal

14 6. Department of Physics, St. Xavier's College, Maitighar, Kathmandu, Nepal

15

16

17 **Abstract**

18

19 In this study, we analyze the climatology of ionosphere over Nepal based on GPS derived VTEC
20 observed from four stations: KKN4 (27.80° N, 85.27° E), GRHI (27.95° N, 82.49° E), JMSM
21 (28.80° N, 83.74° E), DLPA (28.98° N, 82.81° E) during years 2008 to 2018. The study
22 illustrates the diurnal, monthly, annual, seasonal and solar cycle variations of VTEC during all
23 time of solar cycle 24. The results clearly reveal the presence of equinoctial asymmetry in TEC
24 which is more pronounced in maximum phases of solar cycle in year 2014 at KKN4 station
25 followed by descending, ascending and minimum phases. Diurnal variation of VTEC showed
26 short-lived day minimum which occurs between 5:00 to 6:00 LT at all the stations considered
27 with diurnal peak between around 12:00 to 15:00 LT. The maximum value of TEC is observed
28 during spring equinox than autumn equinox with a few anomalies. Similarly, winter anomalies
29 are noticed during increasing and maximum phases of the solar cycle 2011 and 2014 from almost
30 all stations taken in the study.

31

32 **1. Introduction**

33 Total electron content (TEC) is a crucial parameter of ionosphere comprising high concentration
34 of electrons and ions, formed under the ionization of extreme ultraviolet (EUV) radiation and
35 solar X-rays. The lower atmospheric disturbance also contributes to ionospheric variability
36 (Anderson and Fuller-Rowell, 1999; Prikryal et al., 2010). A numerous periodic and aperiodic
37 variability identified in the ionosphere makes impact on the applications involving radio link



1 between satellites and ground which play vital role in the communication, navigation and
2 surveillance with important consequences for the reliability and accuracy of the service (Guo et
3 al., 2015). Global positioning system (GPS) is widely used in recent appliances which encounter
4 largest errors in the path due to disturbed ionospheric free electrons which emphasizes to study
5 GPS-TEC variability. The application of GPS technology allows scientists insight into the shape
6 and behavior of ionosphere. List of factors affecting TEC are ionospheric electron density, ion-
7 electron temperature, composition, dynamic vary with altitude, latitude, longitude, local time,
8 seasons, solar as well as magnetic activity. Equatorial ionosphere is being highly vulnerable
9 possess major threats to the communication signals. The ionosphere at mid latitude is less
10 variable hence the most of the observations and measurements are taken from this region where
11 as high latitude ionosphere is sensitive to outer space connected by geomagnetic field lines
12 (Akala et al., 2013; Parwani et al., 2019). Study of VTEC at low-mid ionosphere showed solar
13 activity dependence (Shimeis et al., 2014). TEC has been studied by large number of researchers,
14 Rama Rao et al. (1980) studied the diurnal variation in TEC at Waltair, India and found short
15 lived pre-dawn minimum, a steep early morning rise followed by broad mid afternoon maximum
16 and a steep post sunset fall. The relation between TEC and SSN, $F_{10.7}$ and EUV was studied by
17 Dabas et al. (1993) and pointed out that TEC has nonlinear relation with SSN and linear relation
18 with $F_{10.7}$ and EUV. Ouattara and Amory- Mazaudier (2012) showed solar activity occurring
19 different phases of solar cycle in diurnal variability. Analogous study was carried around the
20 globe using various methods on TEC such as diurnal, monthly, seasonal and solar cycle and solar
21 activity dependency e.g. in South Asia (Chauhan et al., 2011; Walker et al., 1994); in South
22 America (Sahai et al., 2007; Natali and Meza, 2011; Akala et al., 2013; de Abreu et al., 2014);
23 over North America (Huo et al., 2009; Perevalova et al., 2010); in Africa (Shimeis et al, 2014;
24 D'ujanga et al., 2012; Ouattara and Fleury, 2011; Zoundi et al., 2012); over Brazil (Venkatesh et
25 al., 2014a, 2014b, 2015) ; over Japan (Zakharenkova et al., 2012; Mansoori et al., 2016); over
26 China (Guo et al., 2015; Zhao et al., 2007 ; Liu et al., 2013).

27

28 TEC studied at Jet Propulsion laboratory for the year (1998-2008) found stronger annual TEC
29 variation in southern hemisphere and variation in phase and amplitude is more in conjugate
30 hemisphere (Liu et al., 2009). Galav et al. (2010) found semiannual periodicity in daytime TEC,
31 and the spring equinox shows highest TEC and winter solstices the lowest in India. The winter



1 anomaly, semiannual anomaly and annual anomaly are described in paper by Liu and Chen
2 (2009); Rishbeth and Garriott (1998). Global scale TEC research found that the effect on TEC
3 was stronger on day than at night and also at low latitude than in high latitudes. The effect on
4 TEC is seen more on the either side of dip equator than at dip equator (Liu et al., 2009). Parwani
5 et al. (2019) studied latitudinal variation of ionospheric TEC at northern hemispheric region and
6 found that the diurnal TEC has higher value in low than in mid and high latitude and in seasonal
7 variation maximum in Spring and autumn than in summer and winter.

8

9 Many studies on TEC have conducted in Asia, however no result for the climatology of TEC
10 over Nepal for a long-time series, about one solar cycle has been reported up to now. In this
11 paper, we present for the first-time characteristics of ionosphere in Nepal such as the diurnal,
12 annual, seasonal and solar cycle dependence of TEC on the local ionospheric conditions using
13 GPS TEC data obtained from four GPS stations: KKN4, GRHI, JMSM and DLPA. Our study
14 includes GPS TEC data from 2008 to 2018 of the solar cycle 24, including all four phases of this
15 solar cycle, the minimum phase of year 2008-2009; ascending phase of year 2010-2013,
16 maximum phase of year 2014 and descending phase of year 2015-2018. The second section of
17 this paper includes the dataset and methodology, the third for the results and discussion. The
18 concluding remark is discussed in the last section.

19

20

21 **2. Data sets and data analysis**

22 Total electron content (TEC) is total number of electrons integrated along the path from receiver
23 to each GPS satellites which orbits the Earth at altitude of 20,200 km. It measures in TECU,
24 $1\text{TECU} = 10^{16}$ electron/m². The TEC is obtained as (Hofmann-Wellenhof et al., 1992)

$$25 \quad \text{TEC} = \int_R^S N_e(h) dh \quad (1)$$

26 Where, N_e is electron density, R is the receiver altitude and S the satellite altitude. The dual
27 frequency GPS receiver in two L-band of frequency: $f_1 = 1575.42$ MHz and $f_2 = 1227.60$ MHz
28 provide the carrier phase and pseudo-range measurements. The TEC is calculated from these L1
29 and L2 pseudo-range and carrier phase (Hofmann-Wellenhof et al., 1992). Using pseudo-range
30 and phase data, TEC is calculated as

31



1
$$\text{TEC} = \frac{1}{40.3} \left(\frac{f_1^2 f_2^2}{f_2^2 - f_1^2} \right) (P_1 - P_2) \quad (2)$$

2 Where, P_1 and P_2 are the pseudo-ranges for frequencies f_1 and f_2 , respectively.

3 The TEC obtained by this method is called slanted TEC (STEC) which is a measure of the total
4 electron content of ionosphere along the ray path from the satellite to receiver has to be
5 converted to vertical TEC (VTEC) using equation (Titheridge, 1972).

6

7
$$\text{VTEC} = (\text{STEC} - B_s - B_u) \left(\sqrt{1 - \left(\frac{(R_e \times \cos \epsilon)^2}{(R_e + h)^2} \right)} \right) \quad (3)$$

8 B_s and B_u are the biases of instruments of satellites and receivers respectively, ϵ is the elevation
9 angle of satellite and $R_e = 6371$ km is the mean radius of the Earth.

10

11 For this study data was carried out with GPS data taken from four GPS stations: DLPA, JMSM,
12 KKN4 and GRHI from Nepal. The details of the stations including their geographical and
13 geomagnetic coordinates are shown in table 1 and Universal time is considered as all-time
14 references. The GPS data of the four stations were downloaded from www.unavco.org which is
15 freely available to all users. This data is available in RINEX (Receiver Independent Exchange
16 format) v2.1 which is a standard ASCII format. The temporal resolution of this data is 15 min.
17 The raw data is then processed using software developed by Rolland Fleury (Rolland Fleury,
18 July 19, 2018) from Lab-STICC, UMR 6285, Institut Mines-Telecom Atlantique, site de Brest,
19 France which runs on a window operating system to get required TEC.

20

21 The data for solar indices sunspot number (SSN) and solar flux index (F10.7) to study long term
22 solar activity are taken from Royal Observatory of Belgium, Brussels, through website:
23 sidc.oma.be/silso/home and OMNI website <http://omniweb.gsfc.nasa.gov/>. SSN is most
24 consistent solar indices effectively describes solar activities and are valuable mode in forecasting
25 space weather phenomena. The solar flux index provides the information about the total emission
26 produced by the Sun at the wavelength of F10.7 cm at the Earth.

27

28 In this study, we use GPS derived TEC from RINEX file using this method to obtain TEC
29 calibrated at 15 minutes for all measures. Between 30s VTEC sequences, the elevation may vary.
30 This leads to variation in the VTEC depending on the constellation and not just the variation of



1 the content over that period. We have chosen to do the regression over a period 15 minutes with
2 the VTEC obtained displayed in the middle of this period. This makes it possible to have 4 points
3 over 1 hour and therefore to have an evolution of the VTEC 4 times more precise than that of
4 GIM maps which are currently in steps 1 or 2 hours depending on the organization. So, it is
5 better possibility to see and characterize finer local structures in RINEX derived TEC than in
6 GIM.

7 This study analyzes variations of VTEC during different phases of solar cycle 24 along with
8 annual, seasonal and diurnal variation. For this local season classified as winter (November,
9 December, January and February), spring (March and April), summer (May, June, July and
10 August) and autumn (September and October). The classifications of selected years as per solar
11 cycle phases are presented in table 2.

12

13 **3. Results**

14 In this section, we present the signatures of diurnal, monthly, seasonal, solar cycle and
15 geomagnetic variation on GPS VTEC over Nepal which is calculated using Rolland software (as
16 described in sec. 2). Figure 1 represents the position of GPS TEC stations in Nepal used for this
17 study and figure 2 represents the variation of sunspot number and solar flux for the year 2008 to
18 2018.

19

20 **3.1 Diurnal variation**

21 Figure 3a exemplify diurnal variation of VTEC in LT time observed during February 2, 2009,
22 2012, 2014, 2016 and 2017 during the minimum, increasing, maximum and decreasing phases of
23 solar cycle 24 at KKN4 station in Nepal. The plot shows before sunrise ~5:00 LT, VTEC
24 becomes minimum and reaches a maximum around 13:00-14:00 LT and later decreases in the
25 evening and night. The diurnal peak is noticed between 12:00 to 15:00 LT though the peak
26 values change every month. The VTEC plots reveal a growth from dawn to a highest value about
27 5 to 47 TECU after the hours of daylight, it decreases to the lowest value prior to dusk with time
28 difference of ± 1 to 2 hours. A flat curve with minor peaks is identified during minimum and
29 descending phases whereas dome shape with multiple peaks and trough at varying position is
30 observed during ascending and maximum phases. In overall, the VTEC shows a normal trend of
31 diurnal behavior with the lowest value in dawn and dusk and the highest value during the



1 midday. The maximum VTEC in diurnal curve noticed during maximum phases of the solar
2 cycle 2014 then in 2012 the ascending phases and minimum in 2016, 2009 and 2017 during
3 descending and minimum phases. Diurnal variation of VTEC was studied by plotting similar
4 curves for all the days from year 2008 to 2018 for all chosen four stations. In general, the diurnal
5 VTEC behavior exhibits the solar cycle dependency. The diurnal variability of VTEC for all the
6 day is not presented due to constraint of space. In our study the mean diurnal curves for KKN4
7 station of year 2008, 2009, 2010 and 2017 exhibits wave like profile whereas the mean diurnal
8 curves of year 2011, 2012, 2013, 2014, 2015 and 2016 shows parabolic nature which is shown in
9 fig 3b. The similar diurnal profile was noticed for all the stations considered.

10

11 **3.2 Monthly variation in TEC**

12 Figure 4 shows the monthly variability of VTEC for the maximum phase of solar cycle year
13 2014 at KKN4 station. The plot is obtained using average of daily data. The plot shows
14 maximum in equinoctials months (March, April) and minimum in solstices (January). The rise or
15 fall of TEC in each curve follows the diurnal pattern, prominent peak in the midday with
16 different peak amplitude. The lowest VTEC peak observed during January and highest in March.
17 Late afternoon peak noticed in March, June and September whereas the peak centered ~ 2:00 LT
18 for rest of the months. A significant flat peak noticed in December whereas the steep rise in
19 VTEC is noticed in March, April and October. Monthly variation of VTEC was studied by
20 plotting similar curves for all the month from year 2008 to 2018 for all chosen four stations. The
21 plot shows clear wave's activity in mean diurnal curve for year 2008, 2009 and 2010 and from
22 the years 2011 to 2016 the stiff rise in VTEC was noticed and in 2017 the wave activity starts
23 again (plots are not included in this paper).

24

25 **3.4 Seasonal variation in TEC**

26 Figures 5 show two dimensional diurnal plot of VTEC at JMSM station for all the four phases (I
27 minimum-2009, II ascending-2011, III maximum-2014 and IV descending-2015) of the solar
28 cycle 24 which explains how diurnal VTEC varies hourly during four phases. From fig. 5a, 5b,
29 5c and 5d it is observed that equinoctial asymmetry is not noticed in 2009, in 2011 autumn is
30 more intense than spring and in 2014 and 2015 spring VTEC is greater than autumn. In the fig.
31 6a, 6b, 6c, 6d and 6e each panel separately represents the VTEC variation during autumn, spring,



1 summer and winter season for the year 2008, 2009, 2011, 2014 and 2015 at KKN4, GRHI,
2 JMSM and DLPA respectively. The plots show the maximum values of VTEC is ~95 tecu in
3 spring 2014 the maximum year of sunspot cycle and minimum value 10 tecu in 2009 winter the
4 minimum year of sunspot cycle. In the increasing and decreasing phases of solar cycle, the
5 VTEC gradually increases and decreases depending to the amount of UV that arrive the Earth. In
6 general, the plots show that VTEC is maximum during spring followed by autumn, summer and
7 winter, except few cases. Similarly, previous study of GPS TEC for the year 2014 over Nepal
8 also reported the highest value of VTEC on March and lowest on December with distinct the
9 seasonal variations having higher values in spring and lower in winter season (Ghimire et al.,
10 2020). During the sunspot minimum years 2008 and 2009 and 2010, there are no semi-annual
11 variations in the VTEC and it also seems the summer VTEC is as strong as the Autumn VTEC.
12 For the years 2011 to 2016 the semi-annual variations are noticed. During the year 2017, we
13 observed the same pattern as for the year 2008, 2009 and 2010, the summer VTEC is as strong as
14 the Autumn VTEC. At the station KKN4, the VTEC in autumn is very weak in year 2015 and it
15 is smaller than the VTEC in summer. In year 2011 winter anomaly is noticed at KKN4 whereas
16 GRHI and JMSM winter anomaly is observed in year 2011 and 2014. Winter anomaly is not
17 observed at DLPA. In year 2008 spring VTEC identified more than autumn for GRHI, JMSM
18 and DLPA but less than autumn is observed KKN4. In year 2009 only at JMSM spring noticed
19 greater than autumn. The autumn VTEC is greater than spring for all station in 2011 except at
20 JMSM it equal to spring. Large asymmetry is noticed between spring and autumn in year 2014.
21 In year 2015 the summer peak is higher than autumn. In fig. 7 top left panel represents the
22 variation of VTEC during spring, down left during autumn, top right during summer and bottom
23 right during winter from year 2008 to 2017 at KKN4. In spring the difference in VTEC between
24 high and low solar activity is 65 tecu, in autumn 53 tecu, in summer 45 tecu and in winter 40
25 tecu respectively. In fig. 8 the top panel represents VTEC variability during minimum and
26 increasing phases whereas the bottom panel represents the maximum and decreasing phases of
27 solar cycle 24 using GPS station at GRHI. The plot shows that equinoctial asymmetry is not
28 observable during minimum solar cycle 2008 and 2009, it is clearly distinguishable during other
29 phases of solar cycle. In general, the sunrise time in summer and winter is 5:15 LT and 6:45 LT
30 which are differ by 1.5 hours. During summer 2014, the maximum and minimum TEC observed
31 is 21 and 12 tecu whereas in winter the maximum and minimum tec noticed is 25 and 15 tecu



1 respectively (figure 4). It also seems that during sunrise time in summer the VTEC is linear but
2 during the winter it is steep.

3

4 **3.3 Solar cycle variation of TEC**

5 Figure 9 shows the annual mean values of VTEC, solar flux index and sunspot number during
6 the solar cycle from year 2008 to 2018. The black, blue, green and red color line represents
7 VTEC variation on station KKN4, GRHI, JMSM and DLPA whereas pink and light green color
8 line represents variation in SSN and solar flux index, respectively. The plot shows VTEC
9 gradually begins to increase in 2009 and reaches a maximum in 2014. Then it begins to decrease
10 till 2018 which agrees with the sunspot number and solar flux variation in the same plot. The
11 figure shows that the maximum value of peak of ionization in 2014 about 37 tecu in maximum
12 phase of solar cycle and the minimum value in 2008 about 11 tecu in the minimum phase of solar
13 cycle. The observed VTEC variation corresponds to the amount of UV reach to the Earth.
14 Similarly, the solar flux increases from 2011 onward; the measured VTEC also exhibits highest
15 magnitude for the year 2014. The maximum VTEC value shows a decreasing trend since year
16 2015 to 2018 at all the stations used for this study. It is observed from the graph that average
17 annual VTEC shows better synchronization with SSN and solar flux index.

18

19 **3.4 Effects of geomagnetic activity on TEC**

20 Our discussion has so far been confined to the diurnal, monthly, seasonal and solar cycle
21 variation during solar cycle 24 but the presence of geomagnetic storms indicates solar wind-
22 magnetospheric interaction which originates global disturbances in the Earth's magnetic field as
23 well as in ionospheric TEC. The change of solar and geomagnetic activity during the solar cycle
24 produces variation in all ionospheric parameters (Bremer, 2004). During this study, we find
25 VTEC variation by severe ($Dst \leq -200$ nT), intense (-100 nT $\leq Dst \leq -200$ nT), moderate ($-$
26 50 nT $\leq Dst \leq -100$ nT) and weak (-30 nT $\leq Dst \leq -50$ nT) storms (Gonzalez et al., 1994). We
27 leave their detail study for the future work.

28

29 **4. Discussion**

30

31 **4.1 General background**



1 Since the first survey of the ionosphere by Breit and Tuve in 1926, many surveys have been done
2 with ionosonde to characterize the electron density of the ionosphere mainly the maximum of
3 electronic density of the F2 layer : NmF2 (Rishbeth and Garriott, 1969). Since two decades,
4 GNSS receivers have provided access to the TEC of the ionosphere. NmF2 and VTEC provide
5 information on variations in ionospheric ionization.
6 Solar EUV, UV and X rays are the main source of ionization at low and mid latitudes on the
7 dayside of the earth. Earth's rotation introduces a diurnal variation in ionization. The ionizing
8 rays (EUV, UV and X) are emitted on the sun depend upon the sunspots. The sunspots have a
9 cycle of about 11 years. Ionization of the ionosphere follows this 11-year cycle.
10 Morphological characteristics of the ionosphere based on the NmF2 are known since several
11 decades:
12 - annual and semi-annual variations, with stronger electron densities at the equinoxes (Rishbeth
13 et al., 2000)
14 - winter anomaly in F2 region electron densities with greater daytime electron densities at the F2
15 peak NmF2 in winter than in summer (Rishbeth and Garriott, 1969)
16 - ionospheric equinoctial asymmetry defined as different ionospheric behaviour in the two
17 equinoxes
18 - night maximum of ionization related to the post sunset $\vec{E} \times \vec{B}$ drift (Sastri,1983).
19 In this section, we will discuss our results presented in section 3 at the light of the different
20 physical processes creating the variations in ionization.

21

22 **4.2 Sun radiations and solar cycle**

23 The patterns of the solar cycles play a major role in the solar variability: solar radiation and
24 sunspot number and consequently influence the ionosphere. The solar cycle 24 is the smallest
25 solar cycle since the spatial era (1957), in which peak is noticed in 2014, some few major solar
26 flares were erupted from the Sun in February and October 2014 (Kane, 2002) so the maximum
27 VTEC is noticed in February, October shown in fig. 8. Again from fig. 8, higher value of sunspot
28 and solar flux was reported in February 2011 corresponding to X-class solar flare at which
29 higher value of VTEC noted in station considered.

30 Sharma et al. (2012) studied VTEC variation at Delhi lies near equatorial crest region during
31 year 2007 to 2009 low solar activities and found TEC has a short-lived day minimum between



1 5:00-6:00 LT and gradual increase and reaches its peak value between 12:00 to 14:00 LT. The
2 day minimum was found flat during most of the nighttime hours (22:00 to 06:00 LT). Their
3 results show magnitude of daily maximum TEC decreases since 2007 to 2009 due to decrease in
4 solar flux. They also found TEC seasonal behavior depends on the solar cycle and the largest
5 daily TEC is observed during equinoctial month at Delhi. In 2020, Ghimire et al, studied diurnal
6 variation of TEC at JMJG (Lamjung, Nepal) station for the year 2015 found the minimum in pre-
7 dawn, a steady increase in the early morning followed by afternoon maximum then gradual
8 decrease after sunset the similar pattern is also observed our study.

9 In African sector, Tariku (2015) observed from 2008 to 2009 and high 2012 to 2013 values of
10 VTEC during the low and high solar activity phases. According to their finding, the diurnal
11 VTEC values attained maximum in the time interval of 13:00 to 16:00 LT and the least values
12 are mostly at around 06:00 LT.

13 The similar result is noticed in all considered Nepalese GPS stations during the low solar active
14 phases of solar cycle 24 in Nepal. The maximum diurnal variability in VTEC in 2014 is caused
15 by solar active period confirmed by maximum sunspot number (SSN) and solar flux index
16 (shown in fig. 2), VTEC greater in 2012 due to second maximum in SSN and solar flux and
17 minimum VTEC in 2009 and 2017 supported by minimum SSN and solar flux. The diurnal
18 graphs (fig. 3) show better synchronization of VTEC with SSN and solar flux (fig. 2).

19 In Nepalese ionosphere the diurnal VTEC maximum occurs approximately between 12:00 to
20 14:00 LT. Similar to Delhi station in Nepal, the day minimum was found flat during most of the
21 nighttime hours (22:00 to 06:00 LT). In general, the value of diurnal peak in VTEC is maximum
22 during the spring equinoxes except in 2011 in which autumn VTEC is maximum. As the solar
23 flux decreases from 2008 to 2009, the daily maximum VTEC values show a decreasing trend.
24 The seasonal variation of VTEC shows a semiannual pattern, maximum in equinoxes and
25 minimum in summer and winter. It is evident from the fig. 6c and 6d the semi-annual anomaly is
26 noticed during 2011 and 2014.

27

28 **4.3 Diurnal shape**

29 The observed diurnal VTEC pattern reflects the different solar events signature. The noon bite
30 out profile with asymmetric peaks, parabolic profile and wave profile with morning, evening and
31 night peaks and few complex structures are noted in diurnal profile. The quiet day activity at



1 minimum phase, the fluctuating activity during increasing phase, shock activity during maximum
2 phase and recurrent activity during declining phase was noticed in the study of ionospheric
3 parameters at Ouagadougou ionosonde station data in West Africa by Ouattara et al. (2009). In
4 mean diurnal curve of year 2008, 2009, 2010 and 2017 the wave like profile and from 2011 to
5 2016 the parabolic profile were noticed in Nepalese VTEC (figure 3b).

6

7 **4.4 Semiannual variation, equinoctial asymmetry**

8 The important parameter for semiannual variation of ionospheric ionization is the variation in
9 atomic/molecular ratio, i.e. concentration of O/N₂ ratio. At solstice, there is circulation of
10 meridional wind of about 25 m/s in middle and low latitudes from summer to winter hemisphere
11 (Rishbeth et al., 2000). These winds carry nitrogen-rich air produced in summer hemisphere into
12 lower latitudes by upwelling in higher latitudes, reducing O/N₂ ratio. At equinox, there is no
13 prevailing meridional circulation. The ratio O/N₂ depends specially on the horizontal circulation,
14 and its seasonal changes accompany the change in global thermospheric circulation between
15 summer-to-winter pattern around the solstices to a symmetrical pattern at equinoxes. The six
16 possible reasons of seasonal and semiannual variations in F₂ layer discussed by Rishbeth (1998)
17 are: a) The compositional changes due to large-scale dynamical effects in the thermosphere b)
18 Variations in the geomagnetic activities c) Energy of solar wind d) The inputs from lower
19 atmospheric phenomena such as waves and tides e) change in atmospheric turbulence and f)
20 Anisotropy of solar and EUV emission in solar latitude (Burkard, 1951).

21 In 2020, Ansari et al. found the minimum value of TEC in January and that becomes maximum
22 in April then decreases in June-July and followed by increase in magnitude of second maximum
23 in September-October and later decrease down till December at CHML and JMSM GRHI of year
24 2017. Referring figure 8, our result of semiannual variation shows the minimum value of VTEC
25 is found in January and that becomes maximum in March-April then decreases in June-July and
26 followed by increase in magnitude of second maximum in October-November and later
27 decreases down till December at GRHI of year from 2009 to 2018.

28 The asymmetry between the two equinoxes is due to geophysical parameters as magnetic indices
29 related to geomagnetic activity (Triskova, 1989) and the IMF B_z the interplanetary component of
30 magnetic field (Russell and Mc Pherron, 1973). The equinoctial asymmetry observed in VTEC is



1 explained by i) the axial hypothesis ii) the Russell Mc Pherron (RM) effect and iii) the
2 equinoctial hypothesis (Chaman Lal, 1996; Shimeis et al., 2014).
3 Ouattara and Amory-Mazaudier (2012) made a statistical model of the F2 layer, at equatorial
4 latitudes, based on data obtained during 3 sunspot cycles. This model shows the influence of the
5 different type of geomagnetic activity defined by Legrand and Simon (1989) and the asymmetry
6 of equinoxes due to the magnetic activity. The asymmetry between the two equinoctial peaks is
7 also due to asymmetry of the thermospheric parameters that influence ionosphere as neutral wind
8 and change in composition (Balan et al., 1998)
9 In Nepalese ionosphere features equinoctial asymmetry is distinctly noticed in 2D plots of year
10 2009, 2011, 2014 and 2015 in fig 5b, 5c and 5d, respectively. In year 2009, equinoctial
11 asymmetry is not noticed during low solar activities. But in year 2011, the autumn is intense than
12 spring which is the features of equatorial ionization anomaly (EIA) crest latitude and in year
13 2014 the difference between equinoctial asymmetry is less (spring > autumn) which is again the
14 characteristics of the EIA trough station. And in 2015, the asymmetry very high (spring >
15 autumn) which is the general feature of TEC at all latitude. Our study can conclude that Nepalese
16 ionosphere sometimes show features of EIA crest latitude and sometimes EIA trough station.

17

18 **4.5 Winter anomaly**

19 The winter or seasonal anomaly introduced due to temperature changes (Appleton, 1935), inter
20 hemispheric transport of ionization (Rothwell, 1963), the significant changes in the Sun-Earth
21 distance (Yonezawa, 1959), seasonal variation of O/N₂ concentration (Rishbeth and Setty, 1961;
22 Wright, 1963; Rishbeth et al., 2000; Zhang et al., 2005) and the upward movement of energy
23 flux (Maeda et al., 1986). The winter anomaly is related to solar activity. Tyagi and Das Gupta
24 (1990) and Bagiya et al (2006) have reported absence of winter anomaly in low solar activities at
25 low latitudes. The change in composition of the constituents being identified as cause of the
26 winter anomaly is coined by Rishbeth and Setty (1961). The least VTEC in June solstice (in
27 Northern hemisphere) during the low and high solar activity phase may be due to the asymmetry
28 heating and which result in transport of neutral constituents from summer to winter hemisphere
29 reducing the rate of recombination. The reduction in recombination rate in winter causes the rise
30 of VTEC in winter than in summer. Gupta and Singh (2001) studied TEC over Delhi and
31 concluded that winter anomaly in TEC appears only during higher solar activity. This winter



1 anomaly is due to the closer distance of the Earth from the Sun and the direction of the wind
2 from the summer season to the winter (Shimeis et al, 2014). Krankowsky et al. (1968) and Cox
3 and Evans (1970) separately pointed out that the ratio of O/N₂ become twice in winter than in
4 summer as a result of higher electron loss rate in summer than in winter. Torr and Torr (1973)
5 observed the winter anomaly in foF₂ under different solar activity at the mid latitude of northern
6 hemisphere and similar result was observed in southern hemisphere during high solar activity.
7 Furthermore, they noticed lower solar activities results lower winter anomaly. In general, June
8 solstice anomaly is higher than the December solstice but in earlier, study done at Agra GPS
9 station noticed some abnormalities in the solstice behavior demonstrating higher VTEC in the
10 summer than autumn and winter anomaly with higher VTEC than in summer (Bagiya et al.,
11 2011).
12 In present study the winter anomaly is noticed in 2011 and 2014. At KKN4 station winter
13 anomaly is noticed in the year 2014; at GRHI 2014 and 2016; at JMSM 2014 and 2016. Winter
14 anomaly is not noticed at DLPA (figure 6c and 6d).

15

16 **4.6 Nighttime maximum**

17 The upward $\vec{E} \times \vec{B}$ drift velocity plays an important role in producing the nighttime post sunset
18 enhancement. The average plasma flux required for the enhancement in equatorial latitude found
19 $(2.2 \pm 0.9) \times 10^{12} \text{ m}^{-2}\text{s}^{-1}$ by Jain (1987) in India. In 2015 Tariku, studied pattern of GPS-TEC over
20 African sector during 2008 to 2009 and 2012 to 2013 and found small enhancements in the
21 VTEC in the nighttime ~ between 21:00 to 23:00 LT especially for equinoctial months and then
22 drops again mostly after 23:00 LT. The enhancement was mostly found in equinoctial months
23 during high solar activities and during low solar activities phase in solstice the pre-reversal
24 enhancement was much smaller. A diurnal plot (fig.3) of Nepalese ionosphere shows similar
25 result of pre-reversal enhancement during high solar activities 2012 and 2014 but not during low
26 solar activities of 2009 and 2017.

27

28 **5. Conclusion**

29 This paper investigates the diurnal, monthly, seasonal and solar cycle variations of VTEC at four
30 mid low latitude stations: KKN4 (27.80° N, 85.27° E), GRHI (27.95° N, 82.49° E), JMSM
31 (28.80° N, 83.74° E) and DLPA (28.98° N, 82.81° E) in Nepal.



- 1 The following conclusions are found:
- 2 - The shape of mean diurnal variation of VTEC depends on the solar cycle phases: no diurnal
- 3 peak is observed during minimum and descending phases of the solar cycle whereas a Gaussian
- 4 with different peak amplitude is noticed during ascending and maximum phases of the solar
- 5 cycle.
- 6 - The week ionospheric activities characterized by lower TEC values during minimum and
- 7 strong activities by higher value of VTEC during maximum phase.
- 8 - Day to day variation in VTEC is significant in all the station. The maximum is noticed at
- 9 KKN4 and minimum at DLPA.
- 10 - The study may reveal that diurnal TEC maximizes at around 12:00 LT to 15:00 LT, with
- 11 minimum in the pre-dawn periods.
- 12 - The mean diurnal profile in the year 2008, 2009, 2010 and 2017 exhibit wave like nature
- 13 whereas the parabolic nature is observed in the year 2011, 2012, 2013, 2014, 2015 and 2016.
- 14 - Equinoctial asymmetry in peak is noticed in spring (March, April) and autumn (September,
- 15 October) in which higher is observed during spring.
- 16 -The winter anomaly is observed in all the available stations at the maximum of sunspot cycle
- 17 2014 and in one other station during the year 2011.
- 18 -During the year 2009 of the sunspot minimum the winter anomaly is not observed for all the
- 19 stations. And there is no equinoctial asymmetry i.e. very weak (compare to the year of the
- 20 maximum) except at JMSM.
- 21 -The spring-maximum is smaller than autumn-maximum mainly during years 2011, 2012, 2013
- 22 and also during year 2008 for one station, these years are years of minimum or increasing phase
- 23 of the sunspot cycle.
- 24 -The equinoctial asymmetry is noticed in all the available stations due to difference in the
- 25 F10.7cm for the two equinoxes.
- 26 -It seems that in Nepal for some years there is no semiannual variation, as we observe sometimes
- 27 that summer values are larger than autumn. It is probably a characteristic of Nepal.

28
29

30 **Acknowledgements**

31 We acknowledge www.unavco.org, <http://aiuws.unibe.ch/ionosphere> (CODG),



1 www.ngs.noaa.gov/CORS/Gpscal.shtml, and <http://www.isgi.unistra.fr/>,
2 <http://celestrack.com/GPS/almanar/Yuma/2017/>, website: sidc.oma.be/silso/home and Omni data
3 site <http://omniweb.gsfc.nasa.gov/> for providing RINEX data for TEC, DCB file, Yuma file and
4 data for solar wind parameters and geomagnetic indices for our calculations. The author would
5 like to acknowledge Nepal Academy of Science and Technology (NAST), Nepal for proving
6 PhD scholarship and ICTP, Italy for giving the opportunity to participate in a workshop on Space
7 weather effects on GNSS operations at low latitudes.

8

9



References

- 1
2
- 3 Akala, A. O., Rabi, A. B., Somoye, E. O., Oyeyemi E. O., Adedoye A. B. (2013). The
4 Response of African equatorial GPS TEC to intense geomagnetic storms during the
5 ascending phase of solar cycle 24, *Journal of Atmospheric and Solar-Terrestrial Physics*,
6 **98**, 50–62, doi:10.1016/j.jastp.2013.02.006.
- 7 Ansari, K., Park, K. D., Panda, S. K. (2019). Empirical and orthogonal function analysis and
8 modeling of ionospheric TEC over South Korean region, *Acta Astronautica*, **161**, 313-
9 324, doi:10.1016/j.actaastro.2019.05.044.
- 10 Anderson, D., Fuller-Rowell, T. (1999). The ionosphere, Space environment topics SE-14,
11 *Space Environment Center, Boulder, Report*.
- 12 Appleton, E. V. & Ingram, L. J. (1935). Magnetic Storms and Upper-Atmospheric Ionisation
13 *Nature*, **136**, 548–549.
- 14 Bagiya, M. S., Iyer, K. N., Joshi, H. P., Tsugawa, T., Ravindra, S., Sridharan, R., Pathan, B. M.
15 (2011). Low-latitude ionospheric-thermospheric response to storm time electro
16 dynamical coupling between high and low latitudes, *J. Geophys. Res.*, **116**, AO1303,
17 doi:10.1029/2010JA015845.
- 18 Balan, N., Batista, I. S., Abdu, M. A., Macdougall, J., Bailey, G. J. (1998). Physical mechanism
19 and statistics of occurrence of an additional layer in the equatorial ionosphere, *J.*
20 *Geophys. Res.*, **103**(A12), 29,169–29,181, doi:10.1029/98JA02823.
- 21 Breit, G., Tuve, M. A. (1926). A Test of the existence of the conducting layer, *Phys. Rev.*, **28**,
22 554–575.
- 23 Bremer, J. (2004). Investigations on long-term trends in the ionosphere with world-wide
24 ionosonde observation, *Advances in Space Research*, **2**, 253–258, doi:10.5194/ars-2-253-
25 2004.
- 26 Buonsanto, M. J. (1986). Possible effects of the changing Earth-Sun distance on the upper
27 atmosphere, *S. Pacific, J. Nat. Sci.*, **8**, 58-65.
- 28 Burkard, O. (1951). Die halbjährige Periodic der F2-Schicht-Ionisation, *ArchivMeteorol.*
29 *Bioklim, Wien*, **4**, 391-402
- 30 Chaman Lal (1996). Seasonal trend of geomagnetic activity derived from solar-terrestrial
31 geometry conforms an axial-equinoctial theory and reveals deficiency in planetary
32 indices, *J. Atmos. Terr. Phys.*, **58**, 1497-1506,doi: 10.1016/0021-9169(95)00182-4.
- 33 Chauhan V., Singh, O. P., Singh, B. (2011). Diurnal and seasonal variation of GPS-TEC during
34 a low solar activity period as observed at a low latitude station Agra, *Indian Journal of*
35 *Radio and Space Physics*, **40**, 26-36.



- 1 Cox, L. P., Evans, J. V. (1970). Seasonal variation of the O/N₂ ratio in the F₁ region, *J. Geophys.*
2 *Res.*, **75**, 6271, doi:10.1029/JA075i051p06271.
- 3 D'ujanga, F. M., Mubiru, J., Twinamasiko, B. F., Basalirwa, C., Ssenyonga, T.J. (2012). Total
4 Electron Content Variations in Equatorial Anomaly Region, *Advances in Space Research*,
5 **50**, No. 4, 441–449, doi: [10.1016/j.asr.2012.05.005](https://doi.org/10.1016/j.asr.2012.05.005).
- 6 Dabas R.S., Lakshmi, D. R., Reddy, B. M. (1993). Solar activity dependence of ionospheric
7 electron content and slab thickness using different solar indices, *Pure App. Geophys.*,
8 **140**, 721-728.
- 9 deAbreu, A. J., Fagundes, P.R., Gende, M., Bolaji, O. S., de Jesus, R., Brunini, C. (2014).
10 Investigation of ionospheric response to two moderate geomagnetic storms using GPS-
11 TEC measurements in the South American and African sectors during the ascending
12 phase of solar cycle 24, *Advances in Space Research*, **53** (9), 1313–1328,
13 doi:10.1016/j.asr.2014.02.011.
- 14 Galav, P., Dashora, N., Sharma, S., Pandey, R. (2010). Characterization of low latitude GPS-
15 TEC during very low solar activity phase, *J. of Atmospheric and Solar –Terrestrial*
16 *Physics*, **72**, 1309-1317, doi:10.1016/j.jastp.2010.09.017.
- 17 Ghimire, B.D., Chapagain, N.P., Basnet, V., Bhatt, K. and Khadka, B. (2020). Variation of Total
18 Electron Content (TEC) in the quiet and disturbed days and their correlation with
19 geomagnetic parameters of Lamjung Station in the year of 2015, *Bibechana*, **17**, 123-132
20 DOI: <https://doi.org/10.3126/bibechana.v17i1.26249>
- 21 Ghimire, B. D., Chapagain, N. P., Basnet, V., Bhatta, K. and Khadka, B. (2020). Variation of GPS-
22 TEC Measurements of the Year 2014: A Comparative Study with IRI - 2016 Model.
23 *Journal of Nepal Physical Society*, **6** (1), 90-96, DOI:
24 <http://doi.org/10.3126/jnphysoc.v6i1.30555.90>.
- 25 Gonzalez, W.D., Joselyn, J.A., Kamide, Y., Kroehl, H.W., Rostoker, G., Tsurutani, B.T. and
26 Vasyliunas, V.M. (1994). What is geomagnetic storm? *J. Geophys. Res.*, **99**, 5771-5792,
27 <https://doi.org/10.1029/93JA02867>
28
- 29 Guo, J., Li, W., Liu, X., Kong, Q., Zhao, C., Guo, B. (2015). Temporal-spatial variation of
30 global GPS-derived total electron content, 1999-2013, *PloS ONE* **10**(7) e:0133378,
31 doi:10.1371/journal.Pone 0133378.
- 32 Gupta, J. K. and Singh, L. (2001). Long term ionospheric electron content variations over Delhi,
33 *Ann. Geophys.*, **18**, 1635-1644, doi: 10.1007/s00585-001-1635-8.



- 1 Hofmann-Wellenhof, B., Lichtenegger H., Collins J. (1992). GPS: Theory and Practice,
2 Springer Verlag/Wien, ISBN 978-3-211-82364-6 and 978-3-7091-3298-5 (eBook).
- 3 Huo, X. L., Yuan Y.B., Ou J.K., Zhang K.F., Bailey G.J. (2009). Monitoring the Global-Scale
4 Winter Anomaly of Total Electron Contents Using GPS Data, *Earth Planets and Space*,
5 **61**, 1019–1024, doi: [10.1186/BF03352952](https://doi.org/10.1186/BF03352952).
- 6 Jain, A.R. (1987). Reversal of EXB drift & post sunset enhancement of the ionospheric total
7 electron content at equatorial latitudes, *Indian Journal of Radio and Space Physics*, **16**,
8 267-272.
- 9 Kane, R. P. (2002). Some implications using the group sunspot number reconstruction, *Solar*
10 *Phys.*, **205**, 2, 383-401, doi:10.1023/A:1014296529097.
- 11 Kramkowsky, D., Kasprzak, W.T., Nier, A.O. (1968). Mass spectrometric studies of the
12 composition of the lower thermosphere during summer 1967, *J. Geophys. Res.* **73**, 7291.
- 13 Legrand, J. P., Simon, P.A. (1989). Solar cycle and geomagnetic activity: A review for
14 geophysicists. Part I. The contributions to geomagnetic activity of shock waves and of the
15 solar wind, *Ann. Geophys.*, **7**(6), 565-578
- 16 Liu, G., Huang, W., Gong, J., Shem, H. (2013). Seasonal variability of GPS-VTEC and model
17 during low solar activity period 2006-2007 near the equatorial ionization anomaly crest
18 location in Chinese zone, *Advances in Space Research*, **51**, 366-376, doi:
19 [10.1016/j.asr.2012.09.002](https://doi.org/10.1016/j.asr.2012.09.002).
- 20 Liu, L. B., Wan, W. X., Ning, B. Q., Zhang M. L. (2009). Climatology of the mean total
21 electron content derived from GPS global ionospheric maps, *J. Geophys. Res.*, **114**:
22 AO6308, doi: 10.1029/2009JA014244.
- 23 Liu, L. B., Chen, Y. D. (2009). Statistical analysis of solar activity variations of total electron
24 content derived at Jet Propulsion Laboratory from GPS observations, *J. Geophys. Res.*,
25 **114** :A10311, doi: 10.1029/2009JA014533.
- 26 Mansoori, A. A., Parvaiz A.K., Rafi A., Roshni A., Aslam A.M., Shivangi B., Bhupendra M.,
27 Purohit P.K., Gwal A.K. (2016). Evaluation of long term solar activity effects on GPS
28 derived TEC, *Journal of Physics: Conference Series*, **759**, 012069, doi:10.1088/1742-
29 6596/759/1/012069.



- 1 Natali, M. P., Meza A. (2011). Annual and Semiannual Variations of Vertical Total Electron
2 Content during High Solar Activity Based on GPS Observations, *Ann. Geophys.*, **29**,
3 865–873, doi: 10.5194/angeo-29-865-2011.
- 4 Ouattara, C., Amory-Mazaudier, C., Fleury, R., Lassudrie Duchesne, P., Vila, P., Petitdidier, M.
5 (2009). West African equatorial ionospheric parameters climatology based Ouagadougou
6 ionosonde station data from June 1966 to February 1998, *Ann. Geophys.*, **27**, 2503-2514,
7 doi: [10.5194/angeo-27-2503-2009](https://doi.org/10.5194/angeo-27-2503-2009).
- 8 Ouattara, F., Fleury R. (2011). Variability of CODG TEC and IRI 2001 Total Electron Content
9 (TEC) during IHY Campaign Period (21 March to 16 April 2008) at Niamey under
10 Different Geomagnetic Activity Conditions, *Scientific Research and Essays*, **6**, No. 17,
11 3609–3622.
- 12 Ouattara, F., Amory-Mazaudier, C. (2012). Statistical study of the equatorial F2 layer at
13 Ouagadougou during solar cycles 20, 21, 22 using Legrand and Simon’s classification of
14 geomagnetic activity, *J.Space Weather Space Clim.*, **2**, A19, doi:10.1051/swsc/20122019.
- 15 Parwani, M., Atulkar, R., Mukherjee, S., Purohit, P.K. (2019). Latitudinal variation of
16 ionospheric TEC at northern hemispheric region, *Russian Journal of Earth Sciences*, **19**,
17 ES1003, doi: 10.2205/2018ES000644.
- 18 Perevalova, N. P., Polyakova A.S., Zalozovski A.V. (2010). Diurnal Variation of the Total
19 Electron Content under Quiet Helio-Geomagnetic Conditions, *Journal of Atmospheric
20 and Solar-Terrestrial Physics*, **72**, 997–1007, doi: [10.1016/j.jastp.2010.05.014](https://doi.org/10.1016/j.jastp.2010.05.014).
- 21 Prikryl, P., Jayachandran, P.T., Mushini S.C., Pokhotelov, D., MacDougall, J.W., Donovan E.,
22 Spanswick E., St-Maurice J.P. (2010). GPS TEC, scintillation and cycle slips observed at
23 high latitudes during solar minimum, *Annales Geophysicae*, **28**, 1307-1316, doi:
24 [10.5194/angeo-281307-2010](https://doi.org/10.5194/angeo-281307-2010).
- 25 Rama Rao P. V. S., Nru D., Srirama Rao, M. (1980). Study of some low latitude ionospheric
26 phenomena observed in TEC measurements at Waltair, India, *Proc. Satellite Beacon
27 Symp.*, 57-65.
- 28 *Rishbeth, H., Garriott O.K. (1969). Introduction to Ionospheric Physics, International Physics
29 Series, 14, New York: Academic Press.*
- 30 Rishbeth, H. (1998). How the thermospheric circulation affects the ionospheric F2- layer, *Solar-
31 Terrestrial Physics*, **60**, 1385-1402, doi: 10.1016/S1364-6826(98)000062-5.



- 1 Rishbeth, H., Muller-Wodarg, I.C.F., Zou, L., Fuller-Rowell, Millward, G.H., Moffett, R. J.,
2 Idenden, D. W., Aylward, A. D. (2000). Annual and semiannual variations in the
3 ionospheric F2-layer: II, physical discussion, *Ann.Geophysicae*, **18**, 945-956, doi:
4 [10.1007/s00585-000-0945-6](https://doi.org/10.1007/s00585-000-0945-6).
- 5 Rishbeth, H., Setty, C.S.G.K. (1961). The F-layer at sunrise, *J. Atmos. Terr. Phys*, **20**, 263-276,
6 doi: [10.1016/0021-9169\(61\)90205-7](https://doi.org/10.1016/0021-9169(61)90205-7).
- 7 Rothwell, P. (1963). Diffusion of ions between F layers at magnetic conjugate points, in Proc.
8 International Conference on the Ionosphere, *Institute of Physics and Physical Society*,
9 *London*, 217-221.
- 10 Russell C. T., McPherron R. L. (1973). Semiannual variation of geomagnetic activity, *J.*
11 *Geophys. Res.*, **78**, 92-108, doi:10.1029/JA078i001p00092.
- 12 Sahai, Y., Becker-Guedes F., Fagundes P.R. (2007). Response of Nighttime Equatorial and Low
13 Latitude F-Region to the Geomagnetic Storm of August 18, 2003, in the Brazilian Sector,
14 *Advances in Space Research*, **39**, 1325–1334, doi: [10.1016/j.asr.2007.02.064](https://doi.org/10.1016/j.asr.2007.02.064)
- 15 Sharma, K., Dabas, R.S., Ravindran, S. (2012). Study of total electron content over equatorial
16 and low latitude ionosphere during extreme solar minimum, *Astrophs. Space Sci.*, doi
17 [10.1007/s10509-012-1133-3](https://doi.org/10.1007/s10509-012-1133-3).
- 18 Shimeis, A., Amory-Mazaudier, C., Fleury, R., Mahrous, A.M., Hassan, A. F. (2014). Transient
19 variations of vertical total electron content over some African stations from 2002 to 2012,
20 *Advances in Space Research*, **54**, 2159-2171, doi: [10.1016/j.asr.2014.07.038](https://doi.org/10.1016/j.asr.2014.07.038).
- 21 Tariku, Y.A. (2015). Patterns of GPS-TEC variation over low-latitude regions (African sector)
22 during the deep solar minimum (2008 to 2009) and solar maximum (2012 to 2013)
23 phases, *Earth Planet and Space*, **67**; 35, doi: [10.1186/s40623-015-0206-2](https://doi.org/10.1186/s40623-015-0206-2).
- 24 Titheridge, J. F. (1972). The total electron content of the southern midlatitude ionosphere, 1965-
25 1971, *J. Atmos. Terr. Phys.*, **35**, 981-1001, doi: [10.1016/0021-9169\(73\)90077-9](https://doi.org/10.1016/0021-9169(73)90077-9).
- 26 Torr, M. R., Torr, D. G. (1973). The seasonal behavior of the F2-layer of the ionosphere, *J.*
27 *Atmos. Terr. Phys*, **35**, 22-37, doi: [10.1016/0021-9169\(73\)90140-2](https://doi.org/10.1016/0021-9169(73)90140-2).
- 28 Triskova, L. (1989). The vernal-autumn asymmetry in the seasonal variation of geomagnetic
29 activity, *J. Atmos. Terr. Phys.*, **51**, 111-118, doi: [10.1016/0021-9169\(89\)90110-4](https://doi.org/10.1016/0021-9169(89)90110-4).
- 30 Tyagi T.R., Das Gupta, A. (1990). Beacon satellite studies and modeling of total electron
31 content of ionosphere, *Indian J. of Radio Space Phys*, 424-438.



- 1 Venkatesh, K., Fagundes P.R., de Jesus R., de Abreu A.J., Sumod S.G. (2014a). Assessment of
2 IRI-2012 Profile Parameters by Comparison with the Ones Inferred Using NeQuick2,
3 Ionosonde and FORMOSAT-1 Data during the High Solar Activity over Brazilian
4 Equatorial and Low Latitude Sector, *Journal of Atmospheric and Solar-Terrestrial*
5 *Physics*, **121**, 10–23, doi:10.1016/j.jastp.2014.09.014.
- 6 Venkatesh, K., Fagundes P.R., Seemala G.K., de Jesus R., Pillat V.G. (2014b). On the
7 Performance of the IRI-2012 and NeQuick2 Models during the Increasing Phase of the
8 Unusual 24th Solar Cycle in the Brazilian Equatorial and Low-Latitude Sectors, *J.*
9 *Geophys. Res.*, **119**, 5087–5105, doi :10.1002/214JA019960.
- 10 Venkatesh, K., Fagundes P.R., Prasad D. S. V. V. D., Denardini C.M. , de Abreu A.J., de Jesus
11 R., Gende M. (2015). Day-to-Day Variability of Equatorial Electrojet and Its Role on the
12 Day-to-Day Characteristics of the Equatorial Ionization Anomaly over the Indian and
13 Brazilian Sectors, *J. Geophys. Res.*, **120**, 9117–9131, doi:10.1002/2015JA021307.
- 14 Walker, G. O., Ma J.H.K., Golton E. (1994). The Equatorial Ionospheric Anomaly in Electron
15 Content from Solar Minimum to Solar Maximum for South East Asia, *Annales*
16 *Geophysicae*, **12**, 195–209.
- 17 Wright, J.W. (1963). The F-region seasonal anomaly, *J. Geophys. Res.*, **68**, 4379-4381, doi:
18 [10.1029/JZ068i014p04379](https://doi.org/10.1029/JZ068i014p04379).
- 19 Yonezawa, T. (1959). On the seasonal and non-seasonal annual variations and the semiannual
20 variation in the noon and midnight densities of the F2 layer in middle latitudes II, *J.*
21 *Radio Res. Labs. Japan*, **6**, 651-668.
- 22 Zakharenkova, I. E., Cherniak I.V., Krankowski A., Shagimuratov I.I. (2012). Analysis of
23 Electron Content Variations over Japan during Solar Minimum: Observations and
24 Modeling, *Advances in Space Research*, **52**, 1827–1836, doi: [10.1016/j.asr.2014.07.027](https://doi.org/10.1016/j.asr.2014.07.027).
- 25 Zhang, S.R., Holt, J.M., Anthony, P., Eyken, V., McCready, M., Amory-Mazaudier, C., Fucao,
26 S., Sulzer, M., (2005). Ionospheric local model and climatology from long-term
27 databases of multiple incoherent scatter radars, *Geophys. Res. Lett.*, **32**, L20102,
28 doi.1029/2005GL023603
- 29 Zhao, B., Wan, W., Liu, L., Mao, T., Ren, Z., Wang, M., Christensen, A.B. (2007). Features of
30 annual and semi-annual variations derived from the global ionospheric maps total
31 electron content, *Annals Geophysicae*, **25**, 2513-2527, doi: 10.5194/angeo-25-2513-2007.



- 1 Zou, L., Rishbeth, H, Muller-Wodarg, I. C.F., Aylward, A.D., Millward, G.H., Fuller-Rowell,
2 T.J., Idenden, D.W., Mofett, R.J. (2000). Annual and semiannual variations in the
3 ionospheric F2-layer I Modeling, *Ann. Geophys.*, **18**, 944.
- 4 Zoundi, C., Ouattara F., Fleury R., Lassudrie-Duchesne P. (2012). Seasonal TEC Variability in
5 West Africa Equatorial Anomaly Region, *European Journal of Scientific Research*, **77**,
6 303–313.
- 7
8
9
10
11
12
13
14
15
16
17
18
19
20
21
22
23
24
25
26
27
28
29
30
31



1
2
3
4
5
6
7
8
9
10
11
12
13
14
15
16
17
18
19
20
21
22
23
24
25
26
27
28
29
30
31

Tables Captions

Table 1. The selected GPS stations and their coordinates, the data of which are used in the study

Table 2. Classification of selected years according to the solar cycle phases



List of figures

- 1
2
3 Fig.1. A map of Nepal showing locations of GPs stations used in our study
4
5
6 Fig. 2 Display the variations of sunspot numbers and solar flux for the year 2008 to 2018.
7
8 Fig. 3a. Diurnal variation of vertical TEC in LT at KKN4 GPS station. The black, blue, light
9 green, red and pink color line represent diurnal variation for the year 2009, 2012, 2014, 2016 and
10 2017 respectively.
11
12 Fig. 3b Diurnal variation of vertical TEC in UT at KKN4 GPS station. The first panel represents
13 wave like mean diurnal curves of year 2008, 2009, 2010 and 2017 and the second pan lrepresents
14 parabolic nature of mean diurnal curves of the year 2011, 2012, 2013, 2014, 2015 and 2016. The
15 plots are arrange following on their diurnal profile.
16
17
18 Fig. 4. Monthlyvariation of vertical TEC in LT for each month of year 2014 at KKN4 station.
19
20
21 Fig. 5 (a), (b), (c) and (d). Two dimensional (2D) variation of vertical TEC according to UT at
22 JMSM stations for one of the year of minimum (2009), ascending (2011), maximum(2014) and
23 descending (2015) phases of solar cycle 24.
24
25 Fig. 6. Seasonal variability of VTEC during year 2008,2009,2011,2014 and 2015 for KKN4,
26 GRHI, JMSM and DLPA stations.
27
28 Fig. 7. Mean yearly seasonal variation of VTEC for year 2008 to 2017 at KKN4
29
30 Fig.8.Maximum VTEC variability at GRHI stations during minimum, increasing, maximum and
31 decreasing phases of solar cycle 24
32
33 Fig. 9. Annual mean VTEC variability at KKN4, GRHI, JMSM and DLPA stations with SSN
34 and solar flux during year 2008 -2018
35
36
37
38
39
40



1 Table 1

2

3

| SN | ID | Locations | Geog. Lat. | Geog. Long. | Geom. Lat. | Geom. Long. | Dip Lat. | Local Time (LT) |
|----|------|-------------------|---------------|----------------|---------------|----------------|-------------|--------------------|
| 1 | KKN4 | Kakani, Nepal | 27.80° N | 85.27° E | 18.62°N | 159.41° E | 43.86 | UT+5:45h |
| 2 | GRHI | Ghorahi, Nepal | 27.95° N | 82.49° E | 18.94°N | 156.82° E | 44.25 | UT+5:45h |
| 3 | JMSM | Jomsom, Nepal | 28.80° N | 83.74° E | 19.71°N | 158.06° E | 45.31 | UT+5:45h |
| 4 | DLPA | Dolpa, Nepal | 28.98° N | 82.81° E | 19.94°N | 157.21° E | 46.03 | UT+5:45h |

4

5

6

7

8

9

10

11

12

13

14

15

16

17

18

19

20

21

22

23

24



1 Table 2.

2

| Interval | Years | Solar cycle phases |
|----------|------------------------|--|
| I | 2008, 2009 | The minimum of solar cycle 24 |
| II | 2010, 2011 | The increasing phase of solar cycle 24 |
| II | 2012, 2013, 2014 | The maximum phase of solar cycle 24 |
| IV | 2015, 2016, 2017, 2018 | The decreasing phase of solar cycle 24 |

3

4

5

6

7

8

9

10

11

12

13

14

15

16

17

18

19

20

21

22

23

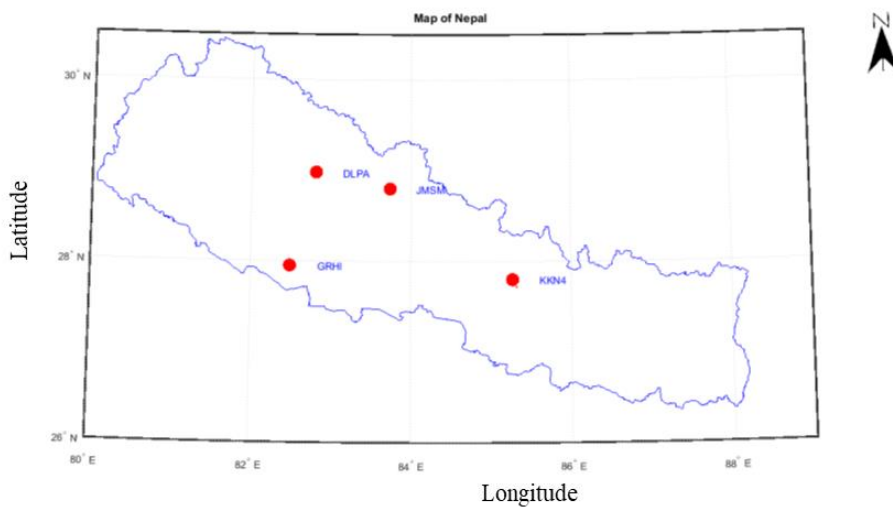
24

25

26



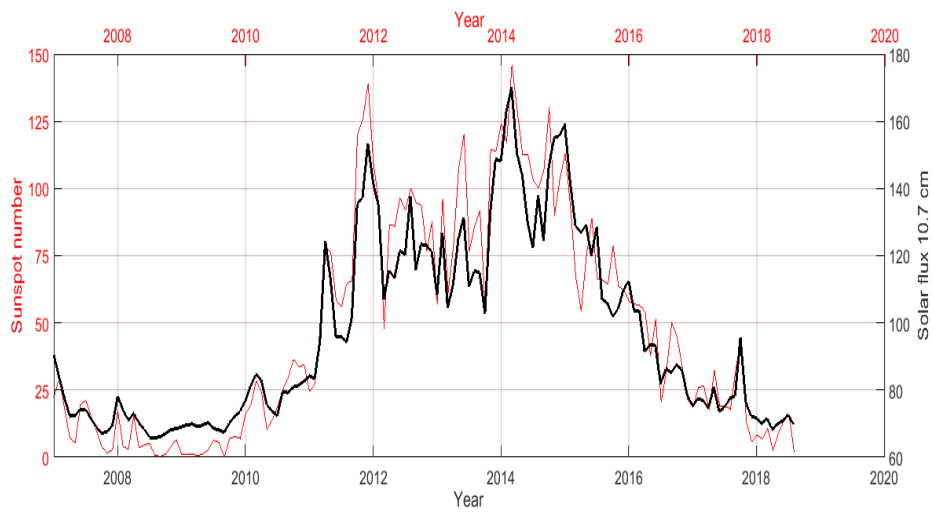
1
2 Figure 1
3



4
5
6
7
8
9
10
11
12
13
14
15
16
17
18
19
20
21



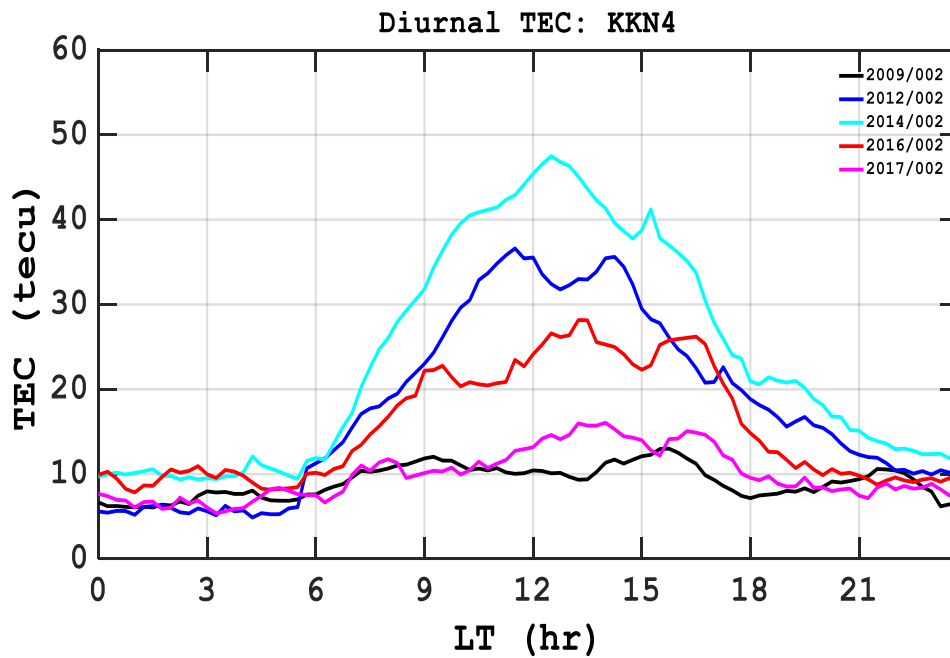
1
2 Figure 2
3



4
5
6
7
8
9
10
11
12
13
14
15
16
17
18
19
20
21



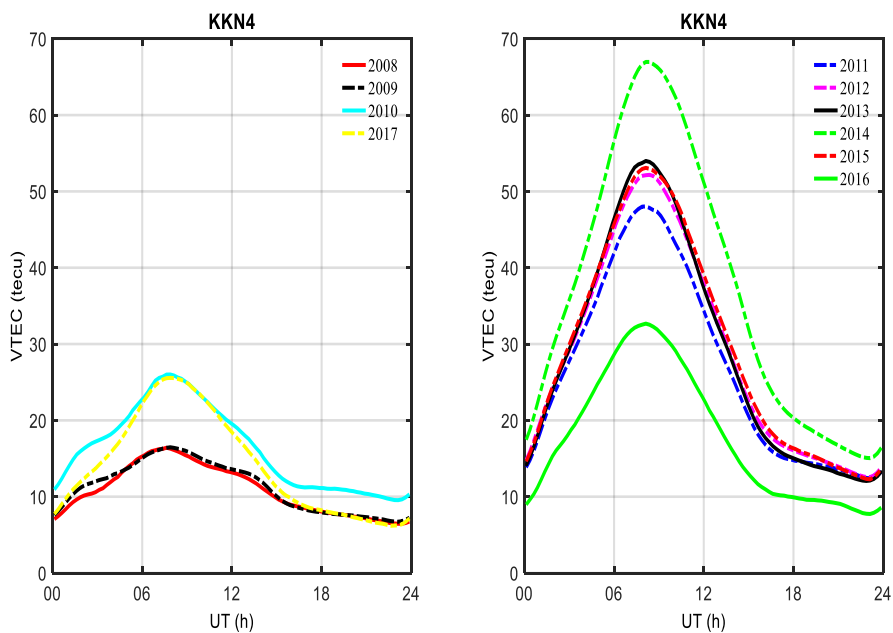
1
2 Figure 3a
3
4



5
6
7
8
9
10
11
12
13
14
15
16
17
18



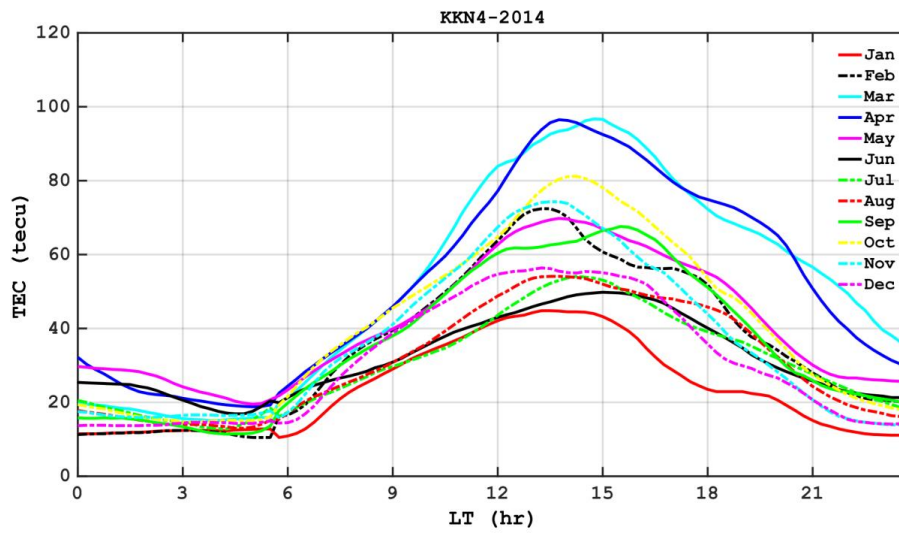
1
2 Figure 3b



3
4
5
6
7
8
9
10
11
12
13
14
15
16
17
18



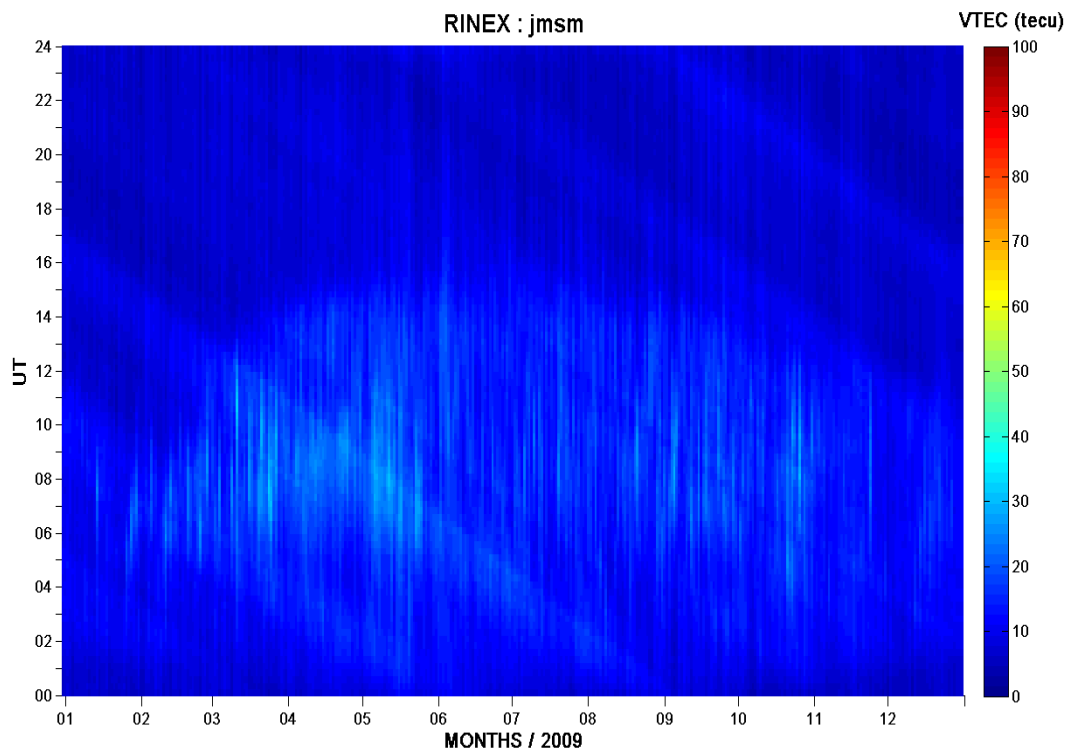
1
2 Figure 4
3
4



5
6
7
8
9
10
11
12
13
14
15
16
17
18
19
20



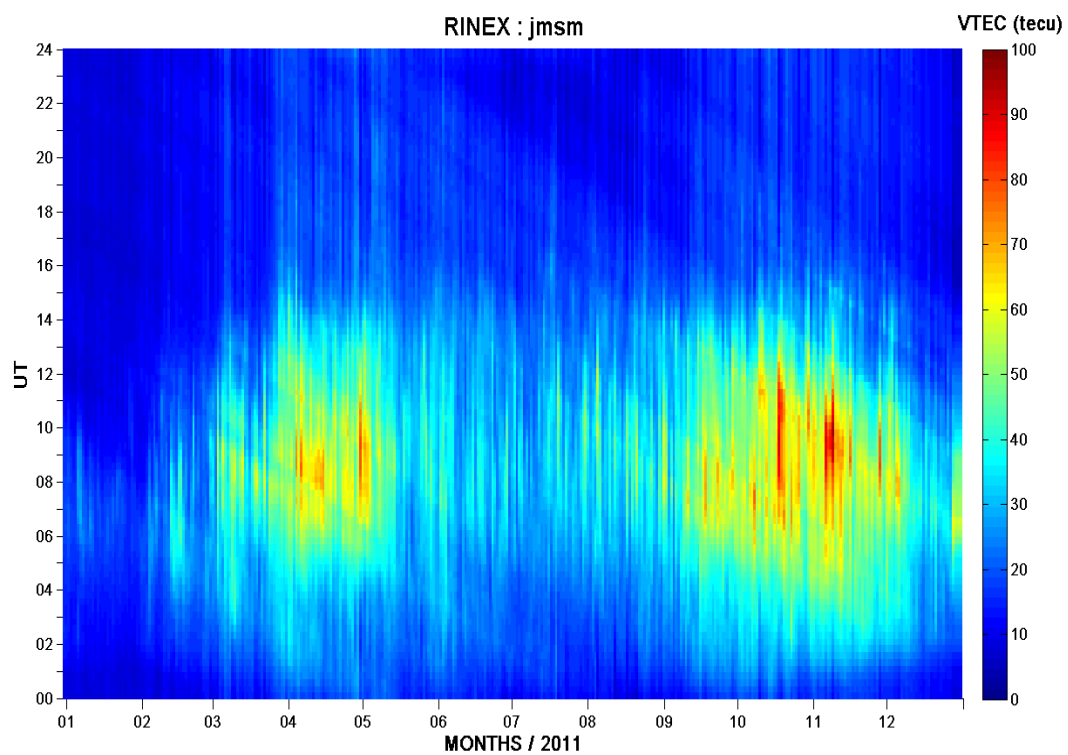
- 1
- 2 Figure 5a



- 3
- 4
- 5
- 6
- 7
- 8
- 9
- 10
- 11
- 12
- 13
- 14
- 15



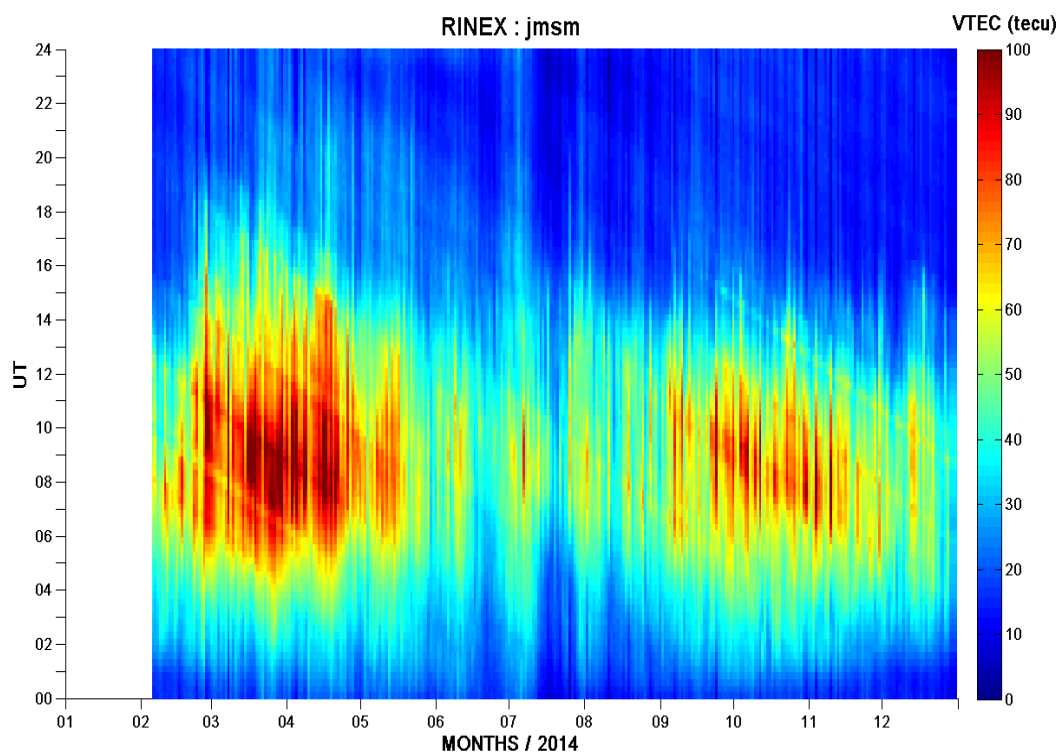
1
2 Figure 5b
3



4
5
6
7
8
9
10
11
12
13
14
15



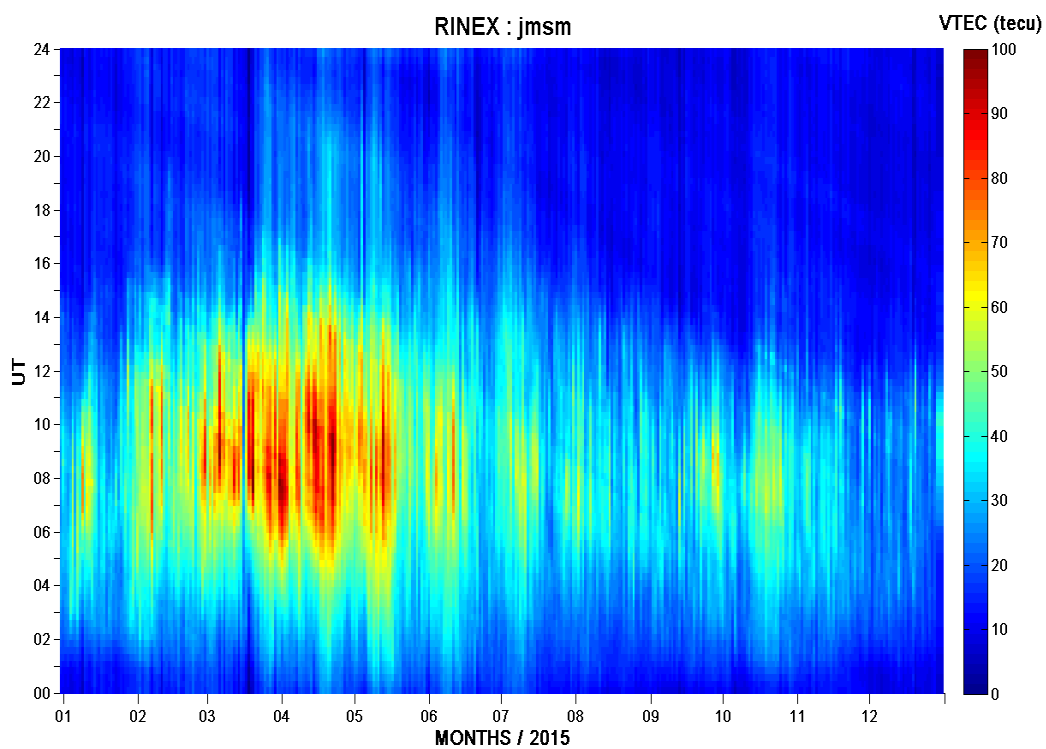
1
2 Figure 5c
3



4
5
6
7
8
9
10
11
12
13
14
15



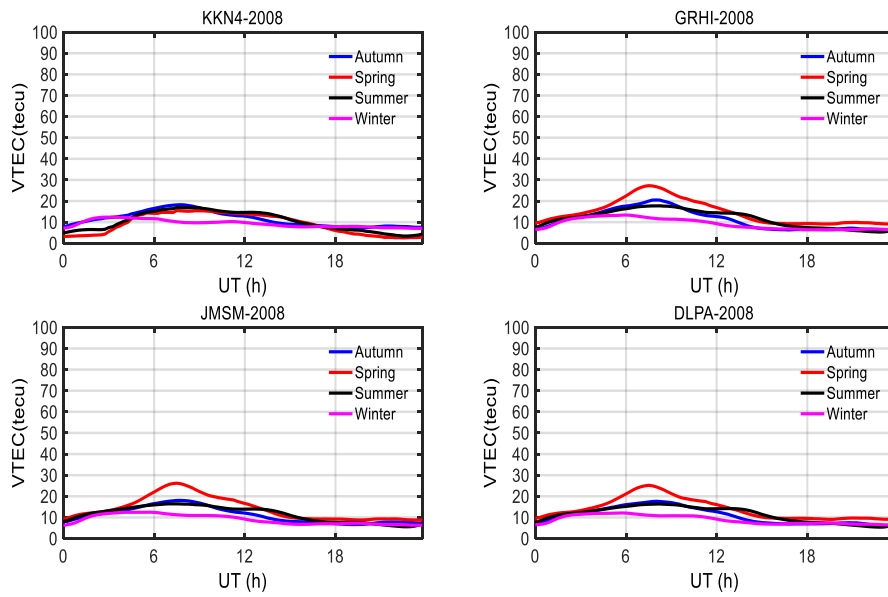
1
2 Figure 5d
3



4
5
6
7
8
9
10
11
12
13
14
15



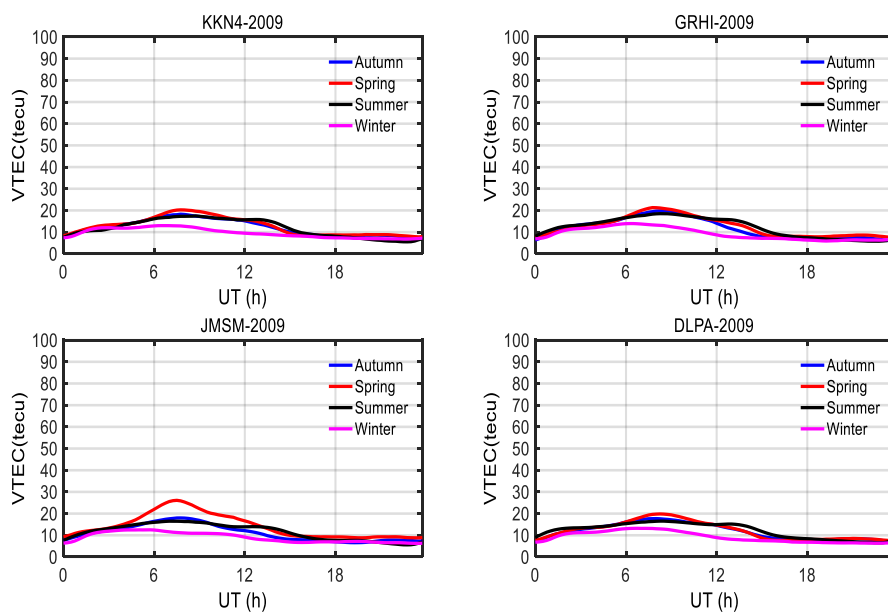
1
2
3 Figure 6a
4



5
6
7
8
9
10
11
12
13
14
15
16
17
18
19



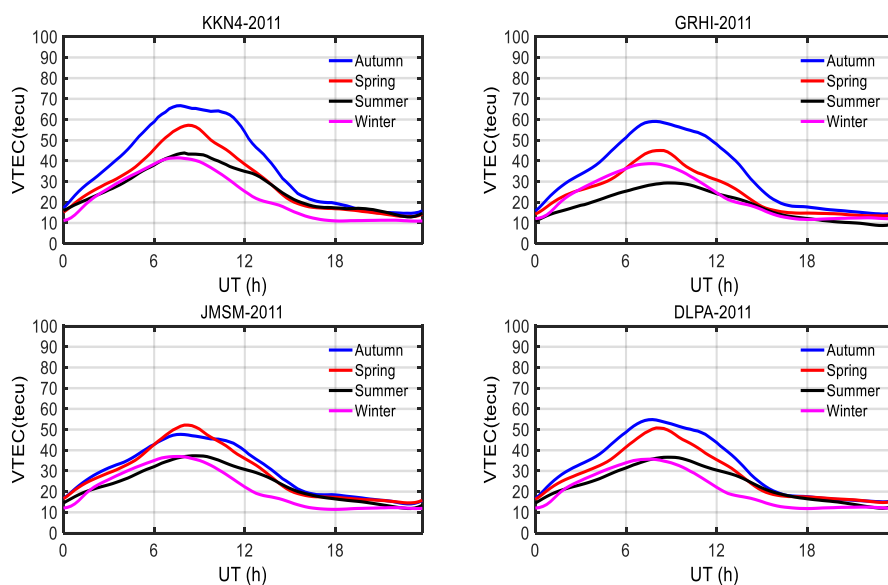
1
2 Figure 6b
3



4
5
6
7
8
9
10
11
12
13
14
15
16
17
18



1
2 Figure 6c
3

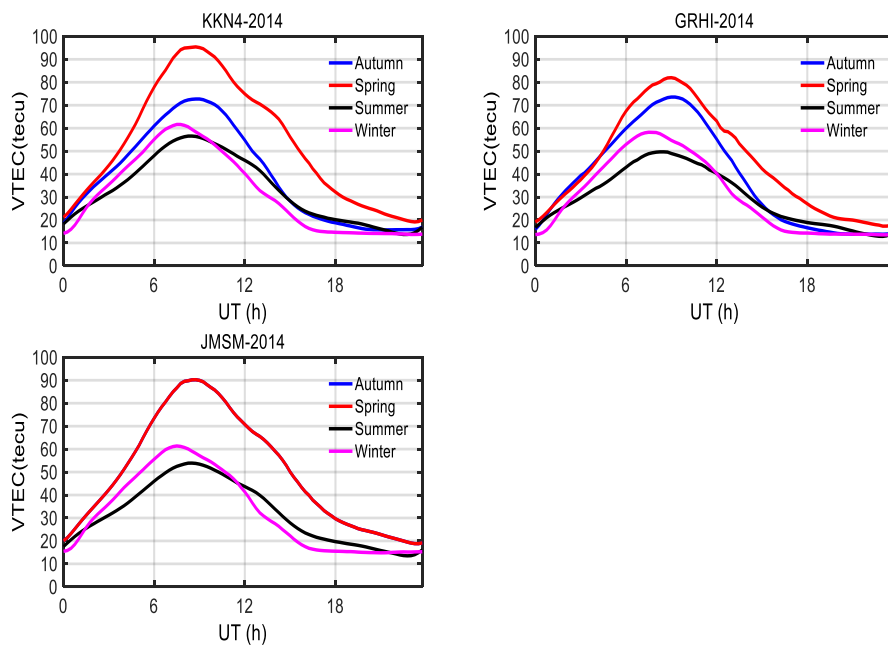


4
5
6
7
8
9
10
11
12
13
14
15
16
17
18
19



1

2 Figure 6d



3

4

5

6

7

8

9

10

11

12

13

14

15

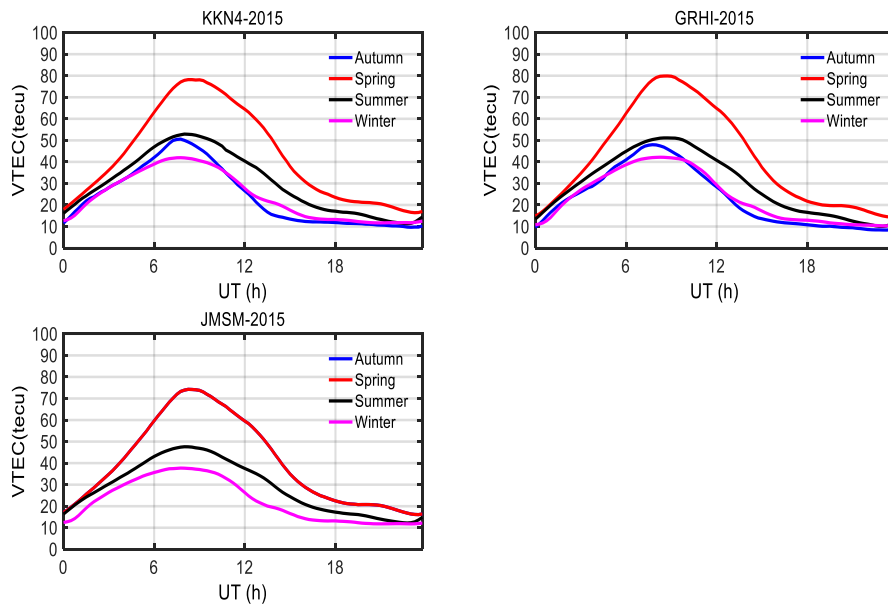
16

17

18



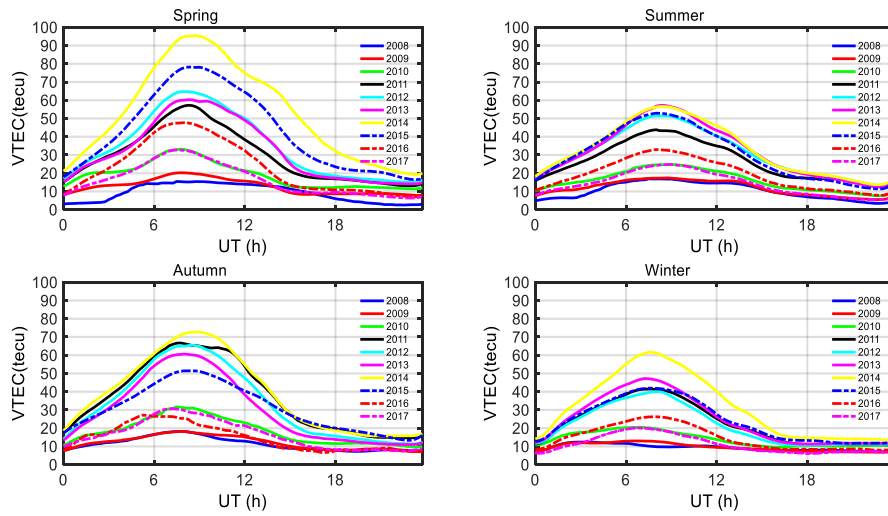
1
2 Figure 6e
3



4
5
6
7
8
9
10
11
12
13
14
15
16
17
18



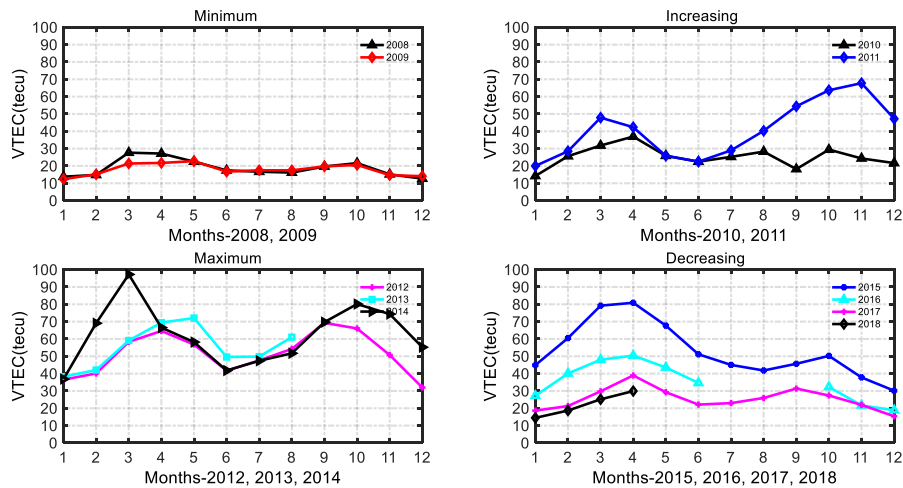
1
2 Figure 7
3



4
5
6
7
8
9
10
11
12
13
14
15
16
17
18
19
20



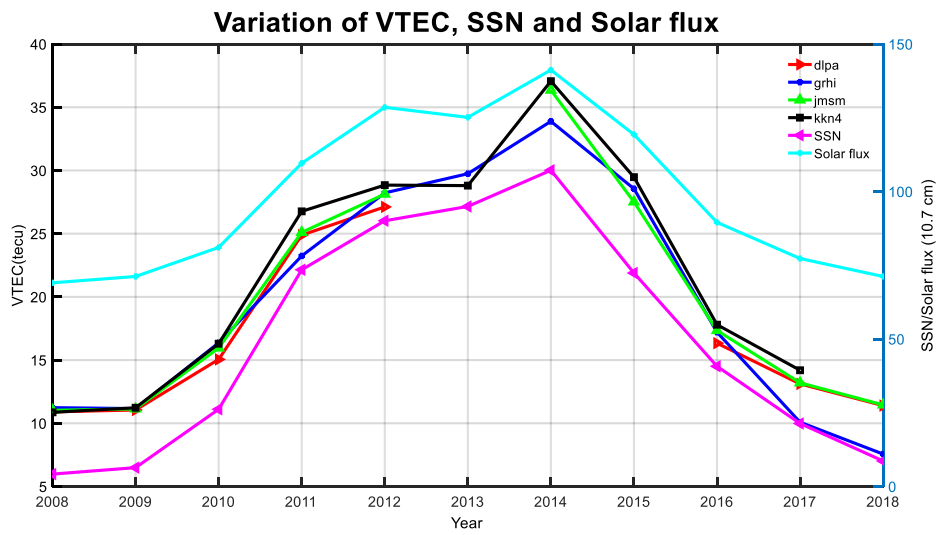
1
2 Figure 8
3



4
5
6
7
8
9
10
11
12
13
14
15
16
17
18
19
20
21



1
2
3 Figure 9
4
5



6
7